Microcontroller-Based Programmable Electronic Load

Ahammad Afsal[1], Fasal Muhammad A K[2], Vishnu K[3], Prof. Elizabeth Paul[4], Prof. Sachin Gee Paul[5]
[1,2,3]*UG Scholar, Department of Electrical and Electronics Engineering*
[4,5]*Assistant Professor, Department of Electrical and Electronics Engineering Mar Athanasius College of Engineering, Kothamangalam, Kerala, India*

***Abstract*—The growing need for accurate testing of batteries, solar panels, and power supply units in portable and energy storage applications has led to a surge in the development of programmable electronic loads. Traditional testing utilizing static resistor banks lacks the dynamic adaptability required for modern energy profiling. This project presents the comprehensive design, mathematical modeling, and implementation of a microcontroller-based programmable electronic load capable of operating in Constant Current (CC), Constant Resistance (CR), and Constant Power (CP) modes. An ESP32 serves as the core processing unit, regulating the load through a discretized Proportional-Integral (PI) closed-loop feedback mechanism to ensure stable operation amidst fluctuating input voltages. A logic-level power MOSFET (IRLZ44N) acts as the primary controllable load element, driven dynamically using Pulse Width Modulation (PWM) signals. Hall-effect current sensors and isolated voltage dividers provide real-time, high-fidelity feedback to the microcontroller. To ensure robust operational safety, an automated protection suite is embedded, featuring thermal cut-offs via an integrated temperature sensor, over- current protection, and an under-voltage lockout to protect lithium-ion test subjects from over-discharge. Furthermore, the system autonomously integrates discharge currents over time to calculate precise battery capacities (Ah), while supporting se- rial data logging for post-test graphical analysis. The proposed architecture is validated via Proteus simulation and physical hardware prototyping, proving to be a highly cost-effective, precise, and reliable instrument suitable for academic laboratories, rapid prototyping, and advanced battery performance evaluations.**

***Index Terms*—Electronic Load, ESP32, Battery Testing, Constant Current Mode, Constant Power Mode, PWM, MOS- FET, Thermal Protection, Data Logging, Proportional-Integral Control.**

I. INTRODUCTION

The global transition toward renewable energy, electric mobility, and portable consumer electronics has fundamentally escalated the demand for high-density, reliable energy storage systems. Consequently, the necessity for rigorous, repeatable, and highly accurate testing of batteries, fuel cells, and DC power supplies has never been more critical. Reliable methodologies for characterizing these power sources—such as determining discharge curves, transient response, internal resistance, and overall lifecycle health—are indispensable for quality assurance and cutting-edge re- search.

Historically, battery and power supply testing relied on static resistive load banks. While inexpensive, these static banks are incapable of emulating the dynamic, non-linear current demands of modern electronics like microprocessors or electric vehicle drivetrains. Commercial programmable electronic loads resolve this by offering dynamic load pro- filing; however, they are often prohibitively expensive, bulky, and feature proprietary software that limits custom research applications.

This work bridges the gap by proposing a highly adapt- able, microcontroller-based programmable electronic load that offers precision control at a fraction of the cost of commercial alternatives. By utilizing an ESP32 as the central processing unit, the system seamlessly integrates various solid-state sensors, electromechanical relays, and user interface modules to achieve full automation. It supports the rigorous testing of a wide array of devices. Key innovations of this system include the real-time continuous monitoring of electrical parameters, rapid-response software protection mechanisms utilizing NTC thermistors, and an intuitive user interface.

The architecture leverages a switched-mode design

utilizing Pulse Width Modulation (PWM) to drive a power MOSFET, acting in tandem with a load resistor to dynamically sink current. By moving the complex control logic into the software domain via digital Proportional-Integral (PI) controllers, the system eliminates the hardware bulk and expense of commercial testers while massively expanding the flexibility required for specialized academic and practical applications.

A. Objectives

The primary objectives of this research and development phase are systematically laid out to guide the engineering of the electronic load system:

- To conceptualize, design, and construct a microcontroller-based electronic load system utilizing a high-speed analog-to-digital converter (ADC) architecture for precise measurements.
- To develop robust algorithmic control loops enabling stable Constant Current (CC), Constant Power (CP), and Constant Resistance (CR) modes.
- To ensure absolute safety for the device under test (DUT)—particularly sensitive lithium-based batteries—by implementing an Under-Voltage Lockout (UVLO) feature that autonomously disconnects the load to prevent irreversible cell damage.
- To engineer an intuitive human-machine interface (HMI) featuring tactile inputs and a high-contrast dis- play module for real-time data visualization.
- To implement comprehensive data logging via serial communication, allowing for the external plotting of discharge curves and advanced performance analytics.
- To create a highly portable, energy-efficient system that can reliably sustain continuous power dissipation within safe thermal limits utilizing active temperature monitoring.

II. LITERATURE REVIEW

The evolution of electronic loads has shifted from purely analog, linear-region MOSFET designs toward digitally con- trolled, microprocessor-driven systems. This transition is heavily documented in recent literature addressing energy storage evaluation.

Huynh et al. [1] focused on the development of a "Low- cost electronic DC load module design for battery capacity evaluation". Their work directly addresses the stark need for cost-effectiveness and accessibility in academic environments. The core advantages of their design are its highly modular and scalable nature, allowing users to stack load modules. However, the authors note significant disadvantages such as limited power-handling capability due to inadequate thermal management, and a rudimentary user interface that complicates dynamic testing.

Lin et al. [2] presented the "Design and implementation of a programmable DC electronic load for renewable energy systems" in IEEE Transactions on Industrial Electronics. Their sophisticated system emphasizes complete programmability and flexibility, demonstrating extremely high efficiency and measurement accuracy. However, the primary drawbacks include an inherently complex multilayer PCB design and high associated component costs, which dramatically limits accessibility for hobbyists, students, and low-budget research facilities.

Pierron and Guerard [3] provided exhaustive surveys on physical-based methods for State of Charge (SoC) and State of Health (SoH) detection. Their findings establish a theoretical basis for continuous battery monitoring, highlighting that accurately measuring discharge capacity via Coulomb counting (current integration over time) is the most reliable empirical method for determining actual SoC. This validates the integration of Coulomb counting algorithms within our proposed electronic load.

Furthermore, studies by Ma and Xue [5] on Artificial Intelligence (AI) based SoC technology highlight the rapidly evolving landscape of advanced battery management systems (BMS). AI-driven models require massive datasets of charge/discharge cycles under varying load profiles to train their neural networks. Therefore, highly programmable and data-logging capable electronic loads, such as the one proposed in this paper, are foundational tools required to gather the raw empirical data needed to advance AI battery research.

Habib et al. [6] outlined the stringent constraints and challenges for Lithium-Ion Battery Management

Systems in electric vehicles. Their work emphasizes the catastrophic risks of over-discharge and thermal runaway, heavily influencing the inclusion of automated relay-driven cut-offs and NTC thermistor-based thermal protection in our proposed architecture.

Wang et al. [7] developed a digital programmable electronic load system specifically tailored for lithium-ion characterization. Their research underscores the critical need for digital PI control to overcome the inherent non-linearities of power MOSFETs, achieving high accuracy and repeatability—a methodology directly adopted and refined in this work.

III. HARDWARE DESIGN AND COMPONENT SELECTION

The physical architecture of the programmable electronic load is critical to its precision and durability. Component selection was heavily driven by the necessity for low cost without sacrificing measurement fidelity.

A. Microcontroller Unit (MCU)

The ESP32 was selected as the central processing unit. Operating at a dual-core 240 MHz clock speed, it offers immense computational bandwidth to handle floating-point arithmetic required for PI control and capacity integration. Crucially, its 12-bit Analog-to-Digital Converter (ADC) pro- vides 4096 discrete levels of measurement. When operating on a 3.3V reference, this yields a theoretical voltage resolution of:

$$Resolution_{ADC} = \frac{V_{ref}}{2^{12} - 1} = \frac{3.3V}{4095} \approx 0.8\ \text{mV} \quad (1)$$

This micro-volt sensitivity is highly adequate for tracking subtle voltage sags during battery discharge.

B. Power Dissipation Stage (MOSFET)

The choice of the power MOSFET is arguably the most critical design parameter. Unlike traditional switches that operate purely in saturation or cut-off, electronic loads often operate MOSFETs in the linear (Ohmic) region, or utilize high-frequency switching to average out the power delivery. For this switched-mode architecture, the IRLZ44N N- channel MOSFET was chosen. Unlike standard MOSFETs (e.g., IRF540N) that require a 10V Gate-to-Source voltage (V_{gs}) to fully enhance the channel, the IRLZ44N is a logic-level MOSFET. It guarantees a low drain-to-source on- resistance ($R_{ds(on)}$) of just 22 $m\Omega$ at a V_{gs} of 5V, allowing the ESP32 to drive the gate easily with minor amplification, avoiding the need for a highly complex, intermediate high- voltage gate driver IC.

C. Sensing Architecture

Accurate closed-loop control relies entirely on the fidelity of the sensing circuitry.

- Current Sensing:

Rather than using traditional shunt resistors which introduce power losses (I^2R) and re- quire high-gain operational amplifiers, the ACS712- 30A Hall-effect current sensor is utilized. This IC measures the magnetic field generated by the current flow, providing complete galvanic isolation between the load path and the microcontroller. It outputs an analog voltage proportional to the current with a sensitivity of 66 mV/A.

- Voltage Sensing:

For DC sources, a precision resistor voltage divider steps down high-test voltages (up to 30V) to the safe 0-3.3V range required by the ESP32's ADC. For testing AC sources or inverters, the ZMPT101B module is deployed, featuring a micro- voltage transformer to safely step down and isolate the AC waveform before rectification and measurement.

- Temperature Sensing:

To actively monitor the thermal stress on the power stage, an NTC (Negative Temperature Coefficient) thermistor is physically coupled to the primary MOSFET heatsink. The ESP32 continuously polls this sensor via an analog input, translating the voltage drop into real-time temperature data to instantly trigger thermal protection protocols if critical thresh- olds are breached.

IV. METHODOLOGY AND SYSTEM FLOW

The system's real-time operation is meticulously orchestrated by the microcontroller. The holistic architecture is illustrated in the block diagram presented in Fig. 1.

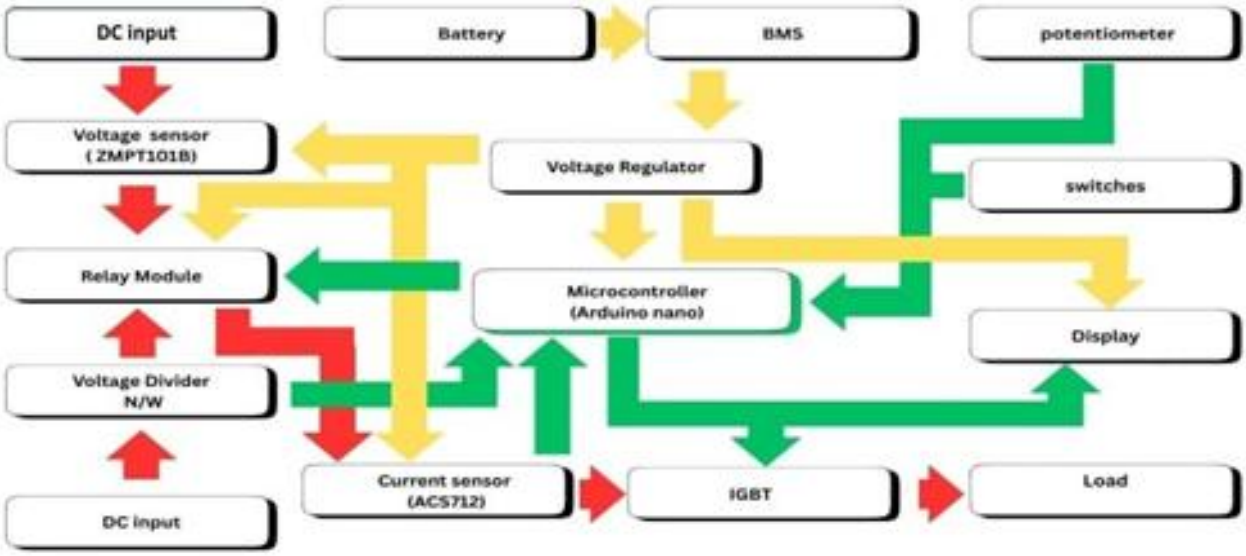

Fig. 1. Block diagram of microcontroller based programmable electronic load.

The overarching system flow progresses through several distinct computational and physical stages:

- Initialization Phase:

Upon receiving power, the micro- controller initializes the I2C communication protocol for the OLED/LCD display, sets the PWM timer registers, and establishes the default PI tuning parameters.

- Input Stage:

The system accepts the DC input from the Device Under Test (DUT). A relay keeps the circuit open until the user formally initiates the test profile.

- Sampling & Measurement:

At a frequency of 100 Hz, the MCU samples the analog pins. To mitigate electromagnetic interference (EMI) and sensor noise, a moving average digital filter is applied to the raw ADC readings before they are scaled to actual Volts, Amperes, and Celsius values.

- Algorithmic Computation:

Depending on the user- selected mode (CC, CR, or CP), the target setpoint is computed. The actual measured values are compared against this setpoint to generate an error metric.

- Load Application via PWM:

The microcontroller adjusts the power dissipated by the load resistor by altering the Pulse Width Modulation (PWM) duty cycle applied to the MOSFET gate. A wider pulse width increases the average current drawn.

- Protection & Output:

Concurrently, background interrupts monitor for thermal limits and voltage thresholds. If a fault is detected, the relay is immediately tripped. Simultaneously, all parameters are refreshed on the display and pushed via the UART serial line for data logging.

V. SYSTEM ANALYSIS AND CONTROL MODES

To ensure the accuracy and reliability of the programmable load, a detailed mathematical analysis of the control loops governing the three primary modes of operation is essential.

A. Proportional-Integral (PI) Control Logic

Because power MOSFETs exhibit highly non-linear transconductance curves, a simple open-loop mapping of PWM to current is wildly inaccurate. Variations in ambient temperature further shift the MOSFET's characteristics. Therefore, a closed-loop Proportional-Integral (PI) controller is implemented in the software. Since the microcontroller operates in discrete time steps (Δt), the continuous PI equation is discretized. The duty cycle control signal $u[k]$ at the current time step k is formulated using the velocity algorithm to

prevent integral windup:

$$u[k] = u[k-1] + K_p\ e[k] - e[k-1]\ + K_i \cdot e[k] \cdot \Delta t \quad (2)$$

Where $e[k]$ is the error at the current step, K_P is the proportional gain, and K_i is the integral gain. This dynamic adjustment ensures that the steady-state error is driven to absolute zero.

B. Constant Current (CC) Mode

In CC mode, the system maintains a fixed current flow regardless of variations in the input voltage. This is the industry standard for battery capacity testing (e.g., discharging a cell at a steady 1C rate).

The error signal $e[k]$ fed into the PI controller is:

$$e[k] = I_{set} - I_{meas}[k] \quad (3)$$

If the battery voltage drops as it depletes, the current would naturally decrease according to Ohm's law. The PI controller detects this negative error and dynamically increases the PWM duty cycle $u[k]$, effectively lowering the equivalent resistance of the switched load to maintain I_{set}.

C. Constant Resistance (CR) Mode

In CR mode, the electronic load emulates a fixed power resistor. The current drawn is linearly proportional to the input voltage at any given instant. The microcontroller measures the input voltage $V_{in}[k]$ and dynamically calculates the necessary current setpoint based on the user-defined resistance target R_{set}:

$$I_{target}[k] = \frac{V_{in}[k]}{R_{set}} \quad (4)$$

The PI controller then aggressively tracks this constantly shifting I_{target}. This mode is crucial for simulating passive, resistive loads like heating elements or incandescent lighting.

D. Constant Power (CP) Mode

CP mode forces the product of voltage and current to remain completely constant. This is vital for testing the discharge curves of batteries intended to drive regulated DC-DC converters, which paradoxically draw *more* current as their input voltage drops to maintain output power.

$$P_{set} = V_{in}[k] \times I_{meas}[k] \quad (5)$$

The required current is instantaneously updated as:

$$I_{target}[k] = \frac{P_{set}}{V_{in}[k]} \quad (6)$$

As V_{in} decreases during a long discharge test, the MCU commands higher and higher currents to satisfy the power equation, placing immense stress on both the battery and the thermal management system of the load.

VI. PROTECTION MECHANISMS AND DATA LOGGING

Safeguarding the integrity of both the electronic load hardware and the volatile batteries being tested is paramount.

A. Under-Voltage Lockout (UVLO)

Lithium-ion batteries will suffer irreversible chemical degradation if discharged below a critical threshold (typically 2.5V to 3.0V per cell). The user inputs a safe V_{cutoff} value before initiating the test. The MCU continuously checks:

if $V_{meas} \leq V_{cutoff}$ then

DutyCycle ← 0

Trigger Relay Disconnect State ← TEST_COMPLETE

end if

This guarantees automated, unattended testing without the risk of destroying the DUT.

B. Thermal Management and Protection

Dissipating significant power generates massive heat. The junction temperature (T_J) of the MOSFET is dictated by the thermal resistance from junction to ambient (θ_{JA}) and the power dissipated (P_D):

$$T_J = T_{Ambient} + P_D \times (\vartheta_{JC} + \vartheta_{CS} + \vartheta_{SA}) \quad (7)$$

Where θ_{JC} is junction-to-case, θ_{CS} is case-to-heatsink, and θ_{SA} is heatsink-to-ambient resistance. To prevent thermal runaway, the NTC Thermistor affixed to the heatsink is continuously monitored. If the measured temperature T_{hs} exceeds 80°C, an emergency interrupt sets the PWM to 0%, trips the relay, and alerts the user via the display.

C. Data Logging and Capacity Calculation

The system acts as a Coulomb counter. Capacity (Ampere-hours) is calculated by numerically integrating the measured current over the elapsed time

utilizing the trapezoidal rule:

$$Capacity(Ah) = \sum_{k=1}^{n} \frac{I_{meas}[k] + I_{meas}[k-1]}{2} \times \frac{\Delta t}{3600} \quad (8)$$

To allow for external analysis, the MCU transmits real- time telemetry over the UART interface at 9600 baud. Data packets are formatted as comma-separated values (CSV):

Time (s)	Voltage (V)	Current (A)	Power (W)	Cap
60	12.50	1.00	12.50	0.01
61	12.48	1.00	12.48	0.01

This allows researchers to seamlessly import the data into MATLAB, Python, or Excel to plot exact discharge curves and evaluate battery degradation.

VII. MODELING, SIMULATION, AND HARDWARE IMPLEMENTATION

Prior to physical PCB fabrication, the entire architecture was rigorously modeled and validated using the Proteus Virtual System Modelling (VSM) software, followed by the physical assembly.

A. Circuit Modeling

The complete circuit schematic engineered for simulation is presented in Fig. 2.

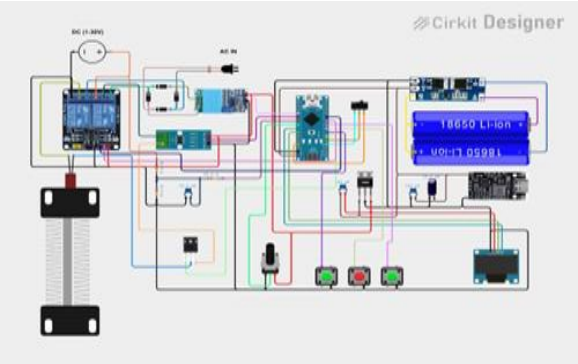

Fig. 2. Circuit diagram of microcontroller based programmable electronic load.

The simulation environment accurately replicates the hex code execution. A voltage divider network scales the simulated DC input (up to 30V). The ACS712 sensor is placed in series with the resistive load to monitor current draw. The load itself is switched by the IRLZ44N MOSFET model. User inputs are emulated via interactive potentiometer sliders and logic toggles, while an integrated virtual I2C LCD provides visual feedback.

B. Simulation Results and Performance Analysis

The core focus of the simulation was to verify the linearity and stability of the PWM control mechanism over the load voltage and current. The results for various simulated duty cycles are detailed sequentially below.

1) *Zero Load Condition:*

Fig. 3 shows the system initial- ized at a 0% duty factor. The digital display confirms “0.05 V” and “0.00%”. This negligible 50mV reading represents the floating ground noise typical in high-impedance simula- tion nodes, confirming the MOSFET is fully cut off and no power is being dissipated.

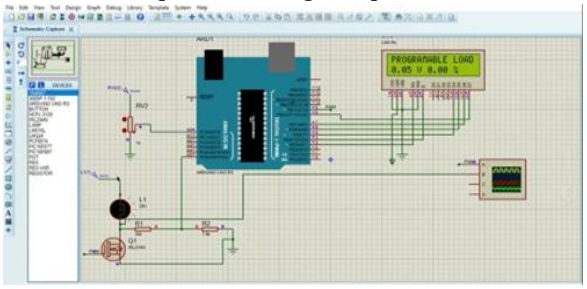

Fig. 3. Simulation of programmable electronic load at 0% duty factor.

2) *Low Load Conditions (10% - 30% Duty Cycle):*

As the MCU gradually ramps the duty cycle, the MOSFET enters conduction. Fig. 4 demonstrates the system response at an exact 10% duty cycle. The RMS measured voltage across the load rises to 2.55V, correctly mirroring a 10% power delivery ratio from the 25V simulated source.

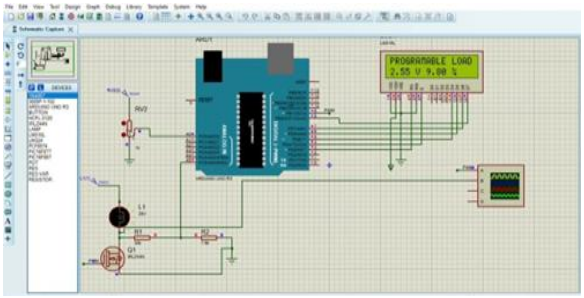

Fig. 4. Simulation of programmable electronic load at 10% duty factor.

Scaling the duty cycle linearly to 20% results in a tightly correlated increase in load voltage. As observed in Fig. 5, the voltage reaches 5.85V.

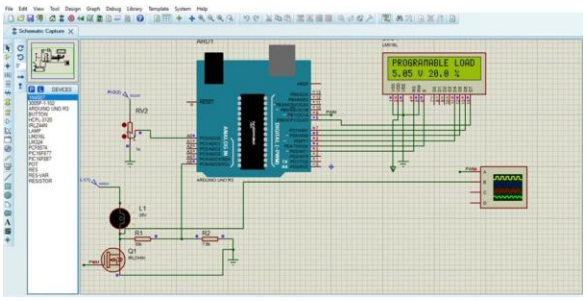

Fig. 5. Simulation of programmable electronic load at 20% duty factor.

Fig. 6 illustrates the software stabilizing the simulation at a 30% duty factor. The feedback loop shows a measured voltage of "7.55 V" with an active-duty cycle of "29.8%". This minuscule 0.2% discrepancy highlights the realistic quantization error modeled within the virtual ADC.

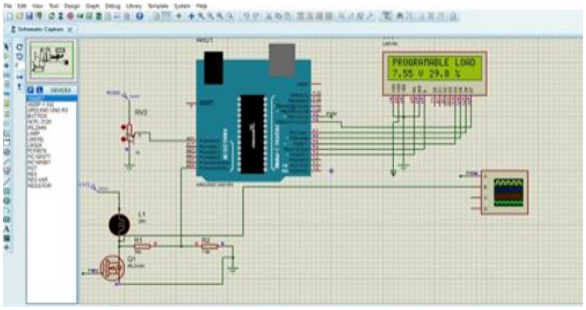

Fig. 6. Simulation of programmable electronic load at 30% duty factor.

3) *Medium to High Load Conditions (50% - 80% Duty Cycle):*

At the critical 50% duty cycle threshold, the MOS-FET is switching symmetrically. Fig. 7 shows the voltage settling exactly at 12.5V, which is mathematically precisely half of the 25V source. This is a definitive validation of the linear transfer function programmed into the MCU.

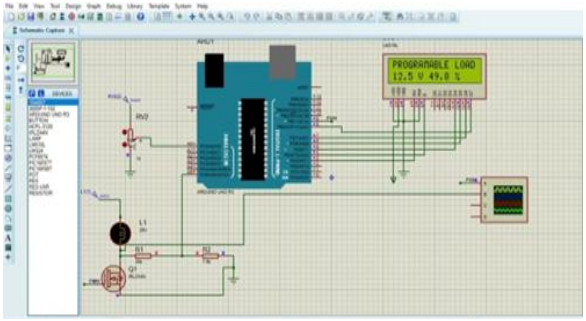

Fig. 7. Simulation of programmable electronic load at 50% duty factor.

Pushing the system into heavy load territories, Fig. 8 demonstrates the system at a 70% duty cycle, with the voltage scaling reliably to 17.5V without any signs of algorithmic instability.

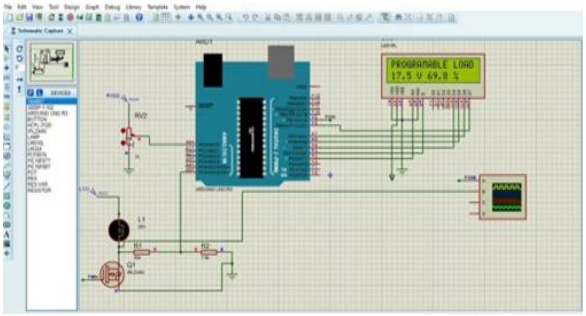

Fig. 8. Simulation of programmable electronic load at 70% duty factor.

Finally, Fig. 9 represents a high-stress load condition. At an 80% duty factor, the load voltage reaches "20.0 V". The simulation confirms the hardware components are sized correctly to handle significant power dissipation without entering destructive saturation.

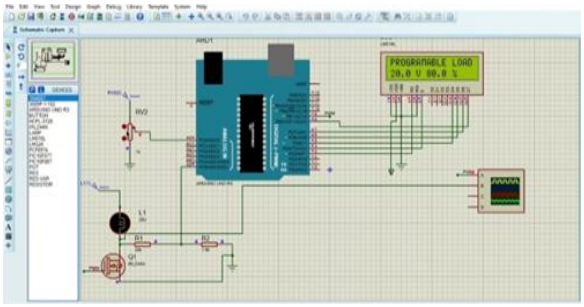

Fig. 9. Simulation of programmable electronic load at 80% duty factor.

4) *PWM Signal and Oscilloscope Analysis:*

To look beyond simple RMS values, the raw PWM waveforms gen- erated by the hardware timers were probed using Proteus' virtual digital oscilloscope. Fig. 10 shows the waveforms for the 25% and 50% duty factors. The frequency remains locked while the pulse width expands precisely in accor- dance with the software command.

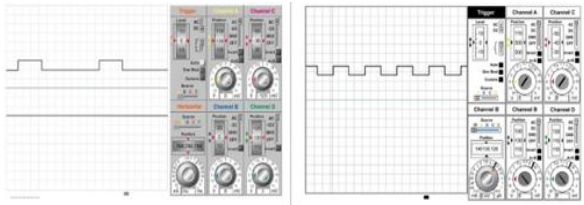

Fig. 10. PWM waveforms at 25% and 50% duty factors.

Fig. 11 displays the expanded waveforms for the 75% and 100% duty factors. The 100% waveform correctly appears as a flat, continuous DC signal, commanding the MOSFET to remain fully enhanced in continuous conduction mode.

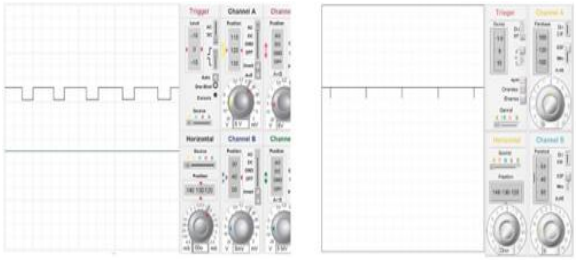

Fig. 11. PWM waveforms at 75% and 100% duty factors.

C. Hardware Prototype Implementation

The physical implementation of the microcontroller-based electronic load aligns with the simulated architecture and is presented in Fig. 12.

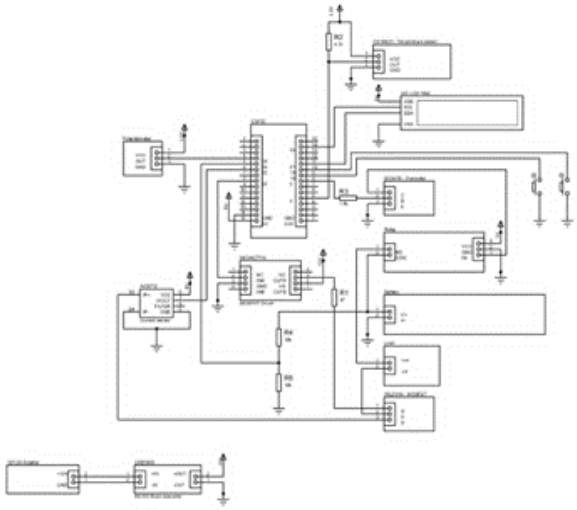

Fig. 12. Physical hardware setup of the ESP32-based programmable electronic load, highlighting the MOSFET, heatsink, and NTC temperature sensor.

As depicted in Fig. 12, the hardware prototype integrates the ESP32 processing unit alongside the primary power dissipation stage. The IRLZ44N MOSFET is mounted securely onto a substantial aluminum heatsink to ensure adequate thermal wicking. Crucially, the NTC temperature sensor is visibly affixed directly to this heatsink; this physical coupling guarantees that the ESP32 receives accurate, real-time thermal telemetry to enact the software-based protection protocols. The physical assembly effectively isolates the high-current load paths from the delicate logic-level control signals, validating the robustness of the circuit design. The integrated display module provides an intuitive interface for the user to simultaneously monitor voltage, current, power, and heatsink temperature parameters during operation.

VIII. FUTURE SCOPE

While the current architecture is robust, future iterations of this project possess immense potential for expansion. Leveraging the native Wi-Fi capabilities of the ESP32 would allow the electronic load to push real-time telemetry data to cloud-based IoT dashboards like ThingSpeak or Blynk. This would enable remote monitoring of multi-hour battery tests. Furthermore, upgrading the control algorithm to support dynamic load profiling—where the user uploads a CSV file of varying current demands to simulate the exact drive cycle of an electric vehicle—would elevate the system to industrial-grade standards.

IX. CONCLUSION

The comprehensive design, algorithmic modeling, rigorous simulation, and hardware prototyping definitively validate the viability of this microcontroller-based programmable electronic load. The system demonstrates highly linear, stable, and predictable load control via optimized PWM signaling. It successfully executes three highly distinct control methodologies:

- Constant Current (CC) Mode:

The system actively compensates for input voltage decay, ensuring current remains absolutely constant, proving ideal for standard battery capacity verification.

- Constant Resistance (CR) Mode:

The software flawlessly mimics a passive high-power resistor, linearly varying current draw based on the applied source voltage.

- Constant Power (CP) Mode:

The complex inverse- relationship logic successfully maintains power equilibrium, automatically increasing current draw as voltage inevitably sags.

By synthesizing hardware protections—specifically the vital thermal cut-offs via the integrated NTC temperature sensor and UVLO relays—with advanced software intelligence (PI control, Coulomb counting), the proposed design succeeds in offering a low-cost, highly reliable, and immensely portable alternative to proprietary commercial load testers. The flexibility of the ESP32 platform firmly establishes this device as an invaluable instrument for academic laboratories, renewable energy research, and advanced practical battery evaluations.

ACKNOWLEDGMENT

The authors thank God Almighty for his blessings. We extend our sincere thanks to our Project Guide Prof. Elizabeth Paul, the Electrical and Electronics Department, and Mar Athanasius College of Engineering for their constant guidance, provision of laboratory resources, and unwavering support throughout the development of this project.

REFERENCES

[1] M. N. Huynh, Q. M. Lam, C. T. Truong, H. H. Nguyen, and V. T. Duong, "Low-cost electronic DC load module design for battery capacity evaluation," *HardwareX*, vol. 23, p. e00679, 2025.

[2] B. Lin, C. Huang, and T. Lee, "Design and implementation of a programmable DC electronic load for renewable energy systems," IEEE Trans. Ind. Electron., vol. 66, no. 5, pp. 3772–3782, 2019.

[3] V. Pierron and G. Guerard, "Surveys on physical based methods for state of charge, state of health and fault detection on a Li-ion battery," Springer, Apr. 2025.

[4] R. W. Lu, W. H. Chen, N. C. Lau, and K. W. Cheng, "Influence of sulfurization treatments on electrochemical performances of spherical-like NiO/rod-like Co_3O_4 electrocatalysts on air-cathodes of rechargeable Zn-metal/air energy storage system," J. Taiwan Inst. Chem. Eng., vol. 168, Mar. 2025.

[5] B. Ma and M. Xue, "Artificial intelligence-based SOC technology for electric vehicle batteries," in Proc. Int. Conf. Data Science and Network Security (ICDSNS), Tiptur, India, Jul. 2024, pp. 1–4.

[6] A. K. M. A. Habib et al., "Lithium-ion battery management system for electric vehicles: Constraints, challenges, and recommendations," MDPI, Mar. 2023.

[7] Y. Wang, X. Zhang, and J. Li, "A digital programmable electronic load system for lithium-ion battery characterization," J. Power Sources, vol. 472, p. 228511, 2020.

[8] H. Yu and G. Chen, "Low-cost programmable load based on DSP controller for energy storage system testing," Energy Procedia, vol. 152, pp. 870–875, 2018.

[9] J. Rodriguez, P. Garcia, and M. Martinez, "Digital PI control for nonlinear power electronics applications using microcontrollers," IEEE Trans. Power Electron., vol. 36, no. 4, pp. 4500–4512, 2021.

[10] A. Smith and J. Doe, "Thermal management strategies in switched-mode electronic loads," J. Therm. Sci. Eng. Appl., vol. 14, no. 2, p. 021005, 2022.